Sensors & Diagnostics

ROYAL SOCIETY OF CHEMISTRY

PAPER

View Article Online
View Journal | View Issue

Cite this: *Sens. Diagn.*, 2022, **1**, 1003

A novel, proof-of-concept electrochemical impedimetric biosensor based on extracellular matrix protein–adhesin interaction†

Juan Leva-Bueno, [a] Ina Meuskens, [b] Dirk Linke, [c] Paul A. Millner [d] and Sally A. Peyman *[ef]

Received 27th April 2022,
Accepted 26th June 2022

DOI: 10.1039/d2sd00075j

rsc.li/sensors

This work presents a novel perspective for electrochemical biosensors based on the detection of the interaction between extracellular matrix proteins and bacterial adhesins. Two types of impedimetric biosensors using collagen as a bioreceptor were investigated for their ability to detect pathogen adhesion using a well-characterised system of collagen-binding to recombinant *E. coli* expressing adhesin. First, a collagen–polymer-matrix-based biosensor was shown to detect whole bacteria in buffer media over the range 8×10^5 cfu to 8×10^7 cfu in a 10 μL sample. Second, a step-by-step full optimised biosensor based on direct collagen attachment showed bacterial detection over the range of 8×10^4 cfu to 8×10^7 cfu in a 10 μL sample. Electrochemical impedance spectroscopy and cyclic voltammetry were employed to assess the binding, which was corroborated by fluorescence binding assays. Up to now, a wide range of bioreceptors have been used in biosensor fabrication, including antibodies, oligonucleotides, phages and molecularly imprinted polymers. In this study, we show that extracellular matrix proteins can also be used for whole pathogen recognition by binding to adhesins.

Introduction

Bacterial infections pose an increasing health risk for humans as antibiotic resistance is on the rise.[1] As antibiotic resistance in bacteria is increasingly common, selection of an effective antibiotic is crucial and therefore accurate, fast diagnostic tools are of utmost importance.[2,3] Biosensors have been developed and shown to be competitive when compared with the current techniques such as ELISA, PCR, SERS and others.[4] However, these techniques are time-consuming and expensive and require specialised personnel to carry out measurements. The advantages offered by biosensors are the miniaturisation of the devices and potential for mass-production, providing lower cost with potentially higher specificity and operation by relatively unskilled users.[5] This is particularly the case for electrochemical biosensors, where the use of screen-printed electrodes (SPE) has allowed miniaturisation *via* modern microelectronics without needing classic bulky electrodes.[6] Impedimetric biosensors are label-free and the working principle consists mainly on surface immobilisation of a bioreceptor, which directly reports on impedance resulting from pathogen binding.[7,8] Due to their sensitivity, biosensors can detect the presence of pathogens in a few minutes, depending on the type of analysis and technique, which is crucial for some post-diagnostic medical interventions.

The most common biosensor configuration comprises a bioreceptor molecule attached to a transducer surface. When the bioreceptor–analyte binding occurs, there is a change in the transducer surface which can be monitored by electrochemical, optical or mechanical means. The choice of bioreceptor component is crucial for the biosensor architecture and fabrication route and strongly depends on the affinity and specificity for the target analyte. Many different types of analytes can be detected, from smallest biomolecules to larger entities such as bacteria and viruses. There are different types of bioreceptors employed for pathogen detection. The use of antibodies as bioreceptors relies on the antibody–antigen interaction, and they are the gold standard of bioreceptors for pathogen detection.[9] There are many reported immunosensors for pathogen detection. A

[a] *School of Biomedical Sciences, Faculty of Biological Sciences, University of Leeds, UK. E-mail: bsjlev@leeds.ac.uk; Tel: +44 (0) 1133433343*
[b] *Department of Biosciences, Section for Genetics and Evolutionary Biology, University of Oslo, Oslo, Norway. E-mail: ina.meuskens@ibv.uio.no*
[c] *Department of Biosciences, Section for Genetics and Evolutionary Biology, University of Oslo, Oslo, Norway. E-mail: dirk.linke@ibv.uio.no; Tel: +47 22857654*
[d] *School of Biomedical Sciences, Faculty of Biological Sciences, University of Leeds, UK. E-mail: P.A.Millner@leeds.ac.uk; Tel: Phone: +44 (0) 1133433149*
[e] *Molecular and Nanoscale Physics Group, School of Physics and Astronomy, University of Leeds, UK. E-mail: S.Peyman@leeds.ac.uk; Tel: +44 (0) 1133433747*
[f] *Leeds Institute for Medical Research, St James' Teaching Hospital, Wellcome Trust Brenner Building, Leeds, LS9 7TF, UK*

† Electronic supplementary information (ESI) available. See DOI: **https://doi.org/10.1039/d2sd00075j**

summary of them can be found in recent reviews either for general[10] biosensors or electrochemical sensors.[11]

Other bioreceptor molecules for pathogen detection are oligonucleotides, DNA or RNA which have been widely used and many examples can be found in the review by Wu *et al.*, 2019.[12] Other bioreceptors include proteins, such as lectins;[13] phage such as those employed for specific bacterial detection using T4 bacteriophages;[14] and sol–gel bacterial imprinted films which have been used for impedimetric detection of *E. coli* by imprinting the bacteria in organosilica films.[15] The concept of using extracellular matrix (ECM) proteins for pathogen detection offers a cheaper option than antibodies and allows detection of groups of pathogens that express adhesins. ECM proteins for pathogen detection in electrochemical biosensors have not been studied extensively although they have been used as bioreceptors for toxin detection.[16] In the present article, an ECM protein, collagen, is presented as a bioreceptor for electrochemical pathogen biosensors that target pathogen borne adhesins.

During an infection, interaction between the pathogenic bacterium and the host cell surface is the first and most crucial step.[17] For adhesion, bacteria express a multitude of surface proteins able to adhere to specific cell surface factors or, more generally, the extracellular matrix.[18] Some of these adhesins are specific for adhesion to only one host cell factor while other adhesins can bind several host cell factors.[17,19] One of these adhesins is YadA, the major adhesin A of *Yersinia enterocolitica*. YadA belongs to the group of

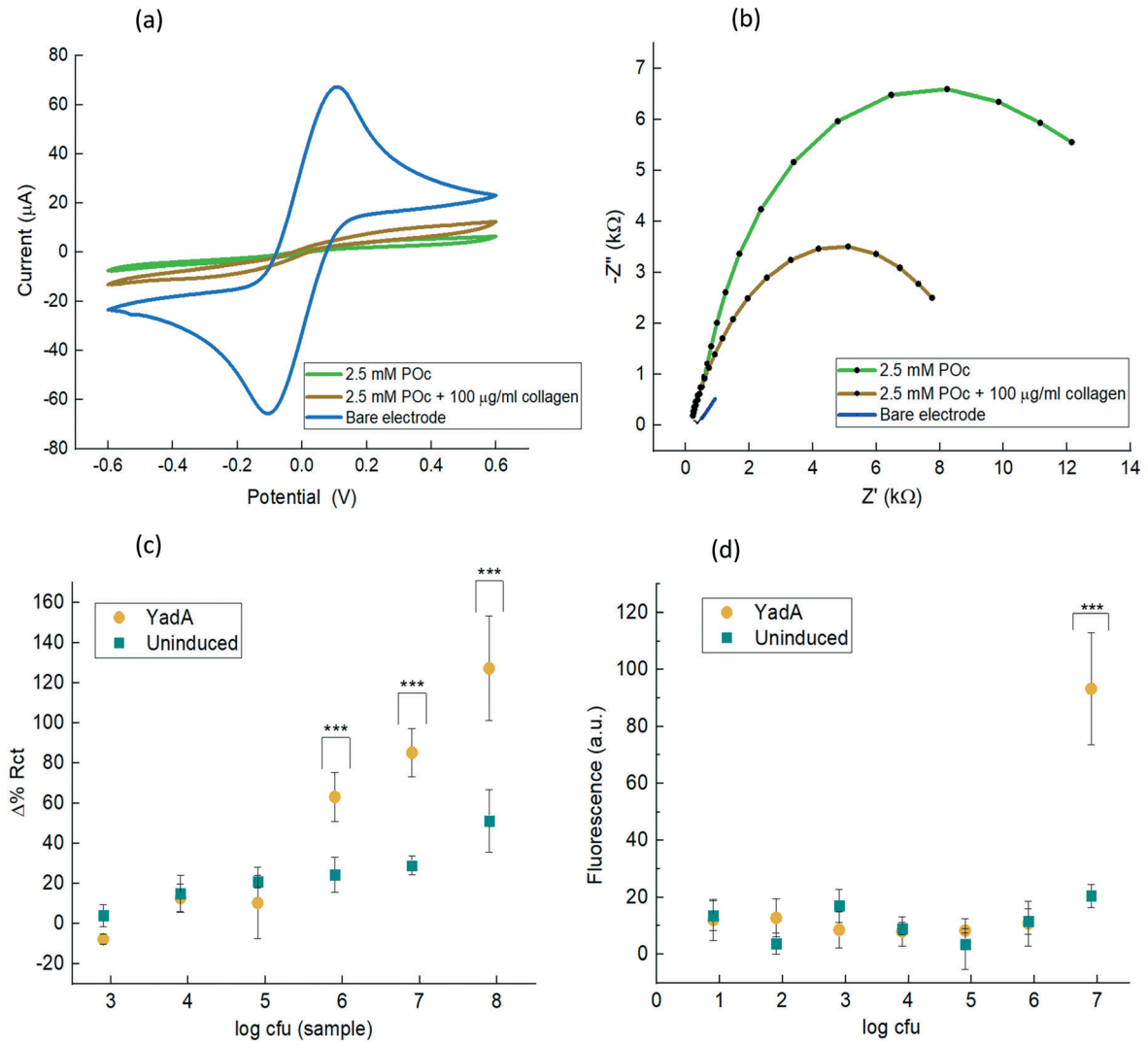

Fig. 1 Electrochemical characterisation of collagen–POc matrix biosensor and bacterial detection. (a), CV voltammogram of bare gold working electrode surface, POc and collagen–POc matrix. The CV was cycled from −0.6 V to +0.6 at a scan rate of 100 mV s^{-1} in 10 mM $[Fe(CN)_6]^{3-/4-}$ in 10 mM PBS, pH 7.2; (b), Nyquist plot of bare, POc and POc + 100 μg mL^{-1} collagen. EIS were carried out in 10 mM $[Fe(CN)_6]^{3-/4-}$ in 10 mM PBS, pH 7.2, frequency of +5 kHz to +0.1 Hz; (c), Δ% R_{ct} before and after analyte incubation with uninduced *E. coli* or *E. coli* expressing YadA. Incubation was for 30 min. Data are mean ± SD ($n \geq 6$); (d), fluorescence assay based on sfGFP – expressing *E. coli* attaching to wells coated with collagen. Fluorescent *E. coli* with or without YadA expression were added to collagen coated wells and fluorescence was measured after washing. Statistical analysis was using ANOVA and data with $p < 0.001$ are indicated by ***.

autotransporter adhesins (type V secretion systems)[20–22] and is a trimeric autotransporter adhesin[23] that is presented on the bacterial surface. It has been shown to bind to a variety of extracellular matrix proteins, including collagen, fibronectin and laminin.[24] In this article we show a proof-of-concept electrochemical biosensor based on ECM protein–adhesin interaction built upon miniaturised disposable screen-printed gold electrodes (SGPEs). In this research we concentrate on the interaction between YadA and collagen,[20,25,26] using collagen as a novel receptor for detection of YadA-expressing bacteria (Fig. 1a).

The characterisation of the biosensors was carried out by cyclic voltammetry (CV) and electrochemical impendence spectroscopy (EIS) and binding monitored by EIS, which is supported by fluorescence assay.

Experimental

Materials

Screen-printed gold electrodes (BVT-AC1.W1.RS.Dw2) from BVT technologies comprised gold working and counter electrodes and an Ag/AgCl reference electrode in a 3-electrode chip. Palmsens4 potentiostat, galvanostat and frequency response analyser (FRA) and PSTrace (5.8) software were from Palmsens BV. A channel multiplexer (MUX8-R2) and an electrode adapter from Palmsens was employed to perform all replicate experiments simultaneously. Na_2HPO_4 and Na_3PO_4; octopamine hydrochloride; tryptone, agar and yeast used to make the microbial culture and broth; calf skin collagen; goat HRP-conjugated anti-rabbit; BSA, casein from powder from bovine milk and TRIS were all purchased from Sigma Aldrich. NaCl was purchased from Fisher Chemical. $K_3Fe(CN)_6$ and $K_4Fe(CN)_6{\cdot}3H_2O$ were purchased from VWR. Rabbit anti-collagen type I from bovine and human was purchased from 2BScientific. 1-Ethyl-3-(3-dimethylaminopropyl)carbodiimide (EDC), enhanced chemiluminescence Pierce (ECL) reagent and sulfo-NHS (*N*-hydroxysulfosuccinimide) and 1 M MES buffer pH 7 were purchased from Thermo Fisher Scientific. Chemiluminescence images were analysed by G:BOX Gel Imaging System (Syngene Ltd.; Cambridge, UK).

Cloning —O:8 FL

For the *pASK-Iba4c* based YadA full length constructs, Gibson cloning was performed. In short: YadA O:8 was PCR-amplified using Q5 polymerase from the plasmid used in ref. 27 using the following primers: 5′-CGACAAAAATCTAGATAAC GAGGGCAAAAAatgactaaagattttaagatcagtgt-3′ and 5′-GCCATT TTTCACTTCACAGGTCAAGCTTAGttaccactcgatattaaatgatgca-3′. These primers have overlaps to *pASK-Iba4c* for later Gibson annealing. *pASK-Iba4c* was linearized in a PCR reaction using Q5 polymerase (New England Biolabs) and the following primers: 5′-CTAAGCTTGACCTGTGAAGT-3′ and 5′-TTTTTG CCCTCGTTATCTAGATT-3′. Both the plasmid and the insert were PCR purified and DpnI (New England Biolabs) digested for 30 min at 37 °C in Cutsmart buffer (New England Biolabs). DpnI was afterwards inactivated by incubation at 80 °C for 10 min. The Gibson assembly was performed with a self-made Gibson mix for 20 min at 50 °C with a 1 : 5 concentration ratio of plasmid to insert. The assembly mix was transformed into TSS competent *E. coli* Top10 and incubated in SOC medium for 1 h at 37 °C. The transformed *E. coli* were plated on LB agar plates with 12.5 μg mL^{-1} chloramphenicol. From this plate, two colonies were chosen, and 5 mL overnight cultures were prepared with plasmids isolated the next day. After Sanger sequencing, the correct plasmid was transformed into fluorescent *E. coli* Top10 (1) and used for further experiments.

Growth of *E coli* and induction of YadA expression

E. coli Top10 pARA_sfGFP (ref. 27) were transformed with vector *pIBA4c_YadA_FL*. The transformants were then streaked out on a plate supplemented with 25 μg mL^{-1} chloramphenicol and a single colony was picked for further experiments. Overnight cultures were grown in 5 mL LB medium supplemented with 25 μg mL^{-1} chloramphenicol. The next morning a subculture was prepared in LB medium supplemented with 25 μg mL^{-1} chloramphenicol and grown at 37 °C in a shaking incubator to an OD_{600} of 0.5. After reaching the required OD600, YadA surface expression was induced by addition of 1 : 10.000 anhydrotetracycline hydrochloride (Abcam, ab145350) (AHTC, 2 mg mL^{-1} stock). Expression was allowed for another 2 h at 37 °C in the shaking incubator. In case of the negative controls, AHTC was omitted. Proper YadA expression was determined by visual inspection of the bacterial aggregation behaviour indicative of YadA surface presentation.[28] After expression, the OD600 was measured again and cfu calculated. The bacteria were diluted to the required cfu in PBS pH 7.4 and immediately used for measurements.

Preparation of collagen solution

Collagen type I bovine was purchased from Thermo Fisher Scientific (A1064401). Collagen was resuspended to a final stock concentration of 1 mg mL^{-1} in 10 mM acetic acid.

Fluorescence-based detection of YadA-expressing *E. coli*

The bacteria were grown as described above. To also induce sfGFP expression from the genome, 0.02% w/v arabinose was added at every step of the growth process. Wells of a 96-well clear plate were coated with 100 μL of a 10 μg mL^{-1} collagen solution. As negative controls, PBS was added to the wells. The plates were incubated at RT for 1 h. After that, the solutions were discarded, and the wells were washed three times with 200 μL PBS and afterwards blocked with 3% w/v BSA in PBS for 1 h at RT. After YadA expression was allowed for 3 h, the OD_{600} was set to 1.0 for both the uninduced and the induced culture and serial 1 : 10 dilutions were performed in 3% w/v BSA in PBS. 100 μL of each dilution was loaded into the plate. Binding of bacteria was allowed for 1 h at RT under static conditions. After that the wells were washed 3

times with PBS and fluorescence was measured. The measurements were performed in a Synergy H1 plate reader with excitation at 455 nm and an emission 533 nm at gain setting of 100.

Collagen–POc matrix-based biosensor fabrication

SPGEs (BVT-AC1.W1.RS.Dw2) from BVT technologies were employed for biosensor fabrication. Prior to electrochemical measurements, the electrodes were pre-treated in 97% v/v ethanol for 30 min, rinsed with deionised water and dried with N_2. Bovine collagen type I was attached onto the electrode surface as a bioreceptor using a protocol provided by ELISHA Systems Ltd: 25 μL of octopamine in 10 mM PB pH 7.2 was mixed with a solution of 200 μg mL^{-1} collagen at a ratio of 1 : 1 and kept in ice, yielding a final concentration of 2.5 mM octopamine and 100 μg mL^{-1}. The final solution was spread across the working electrode and electropolymerised for 2 cycles at a scan rate of 100 mV s^{-1} from +0.0 V to +1.6 V, to entrap the collagen. Finally, once the biosensor was fully constructed and optimised, baseline EIS scans were recorded at 0 V over a frequency range of 5 kHz to 0.1 Hz, with a modulation voltage of +10 mV recording three measurements to ensure signal stabilisation. Then, 10 μL of *E. coli* from stock solutions containing 8×10^2 cfu to 8×10^7 cfu was applied to the working electrodes which were incubated for 30 min. The electrodes were then washed with PBS prior to EIS and CV. This procedure was also carried out for the uninduced YadA *E. coli* control. The blank was conducted with the same procedure as per the analyte and the control but substituting PBS buffer for the bacterial sample (Scheme 1).

Collagen direct attachment biosensor fabrication

SPGEs (BVT-AC1.W1.RS.Dw2) from BVT technologies were employed for biosensor fabrication. Prior to electrochemical measurements, the electrodes were pre-treated in 97% v/v ethanol for 30 min, rinsed with deionised water and dried with N_2. For the collagen direct attachment biosensor, a range of different POc concentrations (1, 2.5, 5, 10, 25, 100, and 250 mM) of octopamine were dissolved in 10 mM PB pH 7.2 and spread across the working electrode and electropolymerised for 2 cycles at a scan rate of 100 mV s^{-1} from +0.0 V to +1.6 V. Then, different collagen concentrations (5, 10, 50, 100, 500, and 1000 μg mL^{-1}) were dissolved in 50 mM MES pH 5.5. To the last, EDC and sulfo-NHS were added to the collagen solution to a final concentration of 2 mM EDC and 6 mM sulfo-NHS and immediately spread over the working electrode to react with the amine reactive groups from the POc. After 2 h of incubation, the electrodes were washed 3 times with 50 mM MES pH 5.5 and a final wash with TRIS buffer in order to block any carboxyl reactive groups. Following biosensor optimisation, samples of *E. coli* induced for YadA expression of 8×10^6 cfu in 10 μL sample were tested for different incubation times (5, 15, 30, 45, and 60 min) at RT. For the best optimised biosensor, blocking agents to avoid non-specific binding were assessed. BSA at 1.5 mg mL^{-1} or 1.5 mg mL^{-1} casein in 10 mM PBS were incubated for 1 h over the electrodes at RT to block non-specific binding sites on the biosensor. After that, electrodes were washed with PBS buffer plus 0.05% (v/v) Tween-20. Then, fully constructed biosensors blocked either with 1.5 mg mL^{-1} BSA and 1.5 mg mL^{-1} casein or non-blocked were tested with 10 μL of sample containing 8×10^6 cfu for both induced and uninduced *E. coli* systems. Finally, once the biosensor was fully constructed and optimised, baseline EIS scans were recorded at 0 V over a frequency range of 5 kHz to 0.1 Hz, with a modulation voltage of +10 mV recording three measurements to ensure signal stabilisation. Then, 10 μL of *E. coli* from stock solutions containing 8×10^2 cfu to 8×10^7 cfu was applied to the working electrodes which were incubated for 15 min. The electrodes were then washed with PBS prior to EIS and CV. This procedure was also carried out for the uninduced YadA *E. coli* control. The blank was conducted with the same procedure as per the analyte and the control but substituting PBS buffer for the bacterial sample (Scheme 2).

Chemiluminescence analysis

Midland blotting technique[29] was performed to validate the presence of collagen in the collagen direct attachment

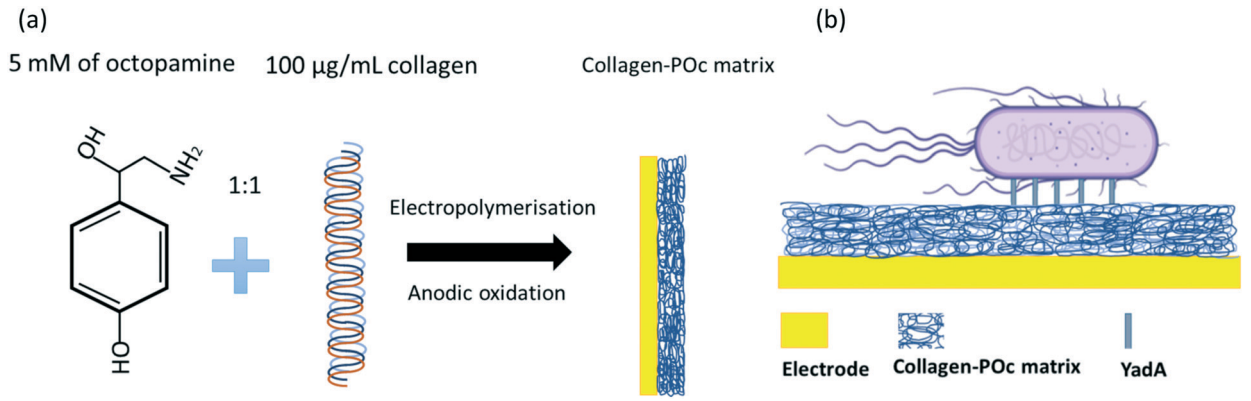

Scheme 1 (a) Schematic representation of step-by-step fabrication of collagen–POc matrix biosensor and (b) final biosensor architecture.

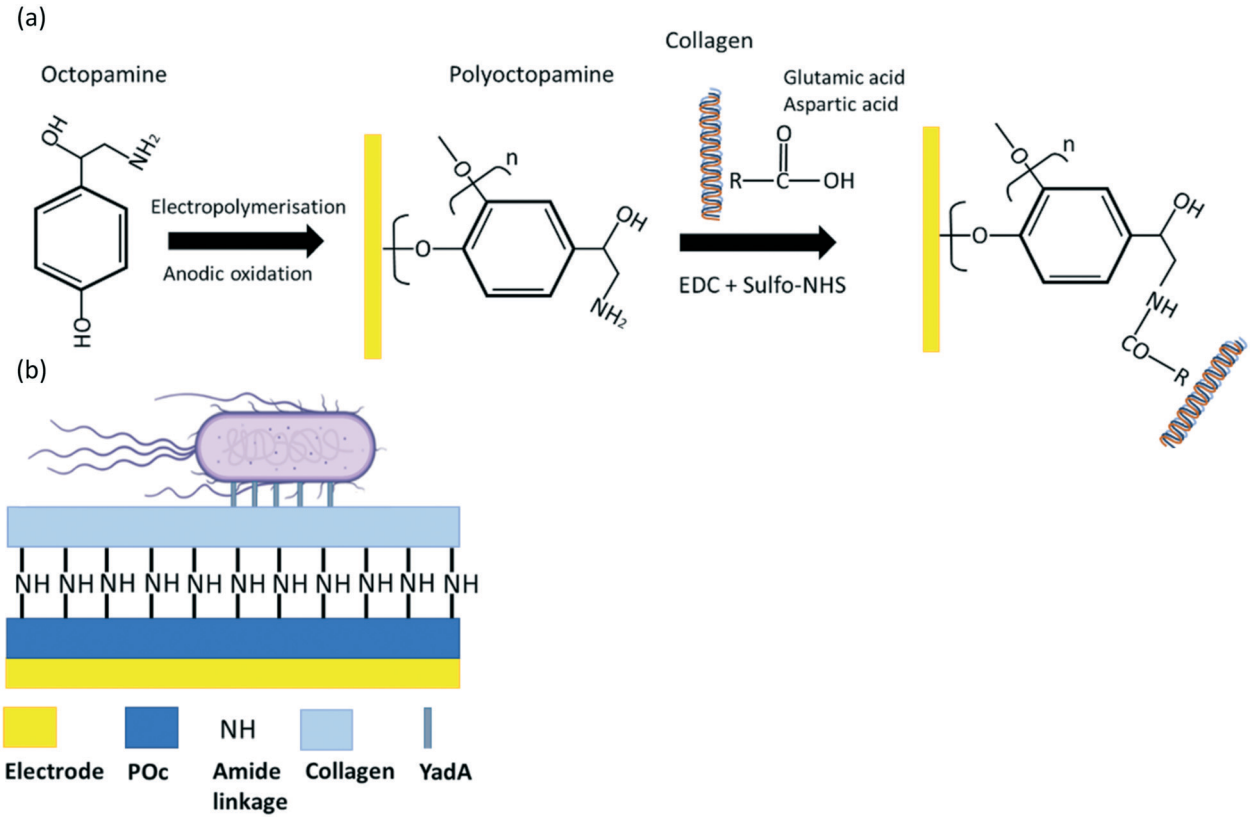

Scheme 2 (a) Schematic representation of step-by-step fabrication of collagen direct attachment biosensor and (b) final biosensor architecture.

biosensor. On-sensor chemiluminescence measurement started with incubation of 1 mg mL^{-1} rabbit anti-collagen type I from bovine and human over the electrode surface. After 1 h incubating in a moist chamber at RT, a washing step with PBS for 5 min was carried out. After that, the electrodes were then incubated with (1 : 1000 in PBS) goat anti-rabbit HRP secondary antibodies for 1 h at RT in a moist chamber. Then the electrodes were washed for 3 times with PBS, for 5 min each time. The second wash with PBS included 0.1% (v/v) Tween-20 to remove non-specific bound material. Finally, ECL reagent was added onto the electrodes to detect the chemiluminescence after 1 min *via* a G:BOX gel Imaging System (Syngene Ltd.; Cambridge, UK).

Electrochemical characterisation and data treatment

The electrodes were subjected to EIS and CV characterisation before and after each step of biosensor construction.

EIS was performed by spreading the electrodes with 10 mM $[Fe(CN)_6]^{3-/4-}$ in 10 mM PBS, pH 7.2, coupled to a potentiostat. EIS was recorded at 0 V over a frequency range of 5 kHz to 0.1 Hz, with a modulation voltage of +10 mV. Three EIS measurements were taken for signal stabilisation at any step of collagen–POc matrix biosensor. Two EIS measurements were taken for signal stabilisation at any functionalisation step in the collagen direct attachment biosensor and 3 EIS measurements before testing the analyte. All EIS analyses were performed in a three-cell system using a Palmsens4 potentiostat, galvanostat and FRA (Palmsens B.V., The Netherlands). PSTrace (5.8) was used for CV and EIS recording. EIS electrochemical circuit fit was assessed with Metrohm Autolab Nova 2.1.4. Data was plotted and analysed in statistical software OriginPro (2019b) and all experiments were replicated with $n \geq 6$.

Frequency response from EIS measurements can be observed in a Nyquist plot which was fit to the Randles' equivalent circuit, from which the charge transfer resistance R_{ct} was obtained. Charge-transfer resistance (R_{ct}) was normalised and expressed in R_{ct} (%) with the eqn (1):

$$\text{Change in } R_{ct}\ (\%) = (R_{ct\ \text{analyte}} - R_{ct\ \text{zero}})/R_{ct\ \text{zero}} \cdot 100 \quad (1)$$

The EIS measurements for signal stabilisation were undertaken keeping the electrode immobile under the electron mediator solution. Since the electrode had to be washed and dried before sampling the bacteria, a blank was recorded by performing the same procedure as per the analyte and control but with just buffer solution.

For CV analysis, the potential was swept between −0.6 V to +0.6 V following for 10 scans at a scan rate of 100 mV s^{-1}.

Results & discussion

Collagen-matrix biosensor

Electrochemical characterisation. Octopamine electropolymerisation was achieved when a characteristic

oxidation peak around 0.6 V was observed for both POc and collagen–POc matrix systems.[30] In the second CV cycle, no oxidative peak was observed. This is indicative that the non-conductive polymer had electropolymerised in the first cycle, impeding the electron flow in the second (Fig. S1a and b†). Once the electropolymerised interfaces were attached to the gold surface, CV was carried out in 10 mM $[Fe(CN)_6]^{3-/4-}$ in 10 mM PBS for each system and compared to a bare surface.

From the voltammograms, the bare electrode showed the two peaks of oxidation and reduction current at clear oxidative and reductive potentials, thus indicating proper electron flow through the metallic surface and presenting a clearly reversible redox reaction. On the other hand, the CV profile shown for POc indicates either oxidative and reductive peak currents of +5.32 μA and −4.17 μA, at +0.3 V and −0.20 V respectively. This shows that once POc is electropolymerised, the redox pair cannot adequately reach the surface to perform exchange of electrons indicating the presence of a non-conducting surface. The collagen–POc matrix voltammogram shows that the observed electrochemical properties are in line with the composition of the interface: the collagen-POc composite presents a more open nanostructure than POc by itself. Consequently, it is easier for the electron carriers to reach the electrode surface and thus presents more conductive properties. The values of the currents achieved were +9.61 μA and −9.93 μA for the oxidative and reductive peaks. This behaviour can be also seen from the electropolymerisation profiles in which less current is observed for the collagen-POc matrix in the oxidative peak compared to only POc (Fig. S1a and b†) (Fig. 1a).

Further assessment through EIS (Fig. 1b) was carried out and the results obtained were in line with what was observed with the CV. The curve obtained for POc was comparatively large when compared to the other systems, as is expected given the insulating effect of the non-conducting polymer. On the other hand, the collagen–POc matrix showed a substantial decrease in impedance compared to POc alone.

Detection of bacteria. To show electrochemical detection of bacteria, a range of YadA-expressing *E. coli* samples were tested. For that, bacteria cfu samples from 8×10^2 to 8×10^7 in 10 μL samples were tested in full constructed biosensor and incubated for 30 min at RT.

The strategy to assess the selectivity of the biosensor consisted of analysing the same range of bacterial samples but for *E. coli* uninduced for YadA expression. Comparison between the analyte and the control was assessed through changes in R_{ct}, which is represented as $\Delta\%$ R_{ct} after normalisation, (Fig. 1c). To obtain the R_{ct} values, each Nyquist plot was fitted into a Randle's equivalent circuit model. The bacterial binding of YadA-expressing *E. coli* appeared significantly different ($p \leq 0.001$) from 8×10^5 cfu to 8×10^7 cfu. For this range of cfu, the response to YadA-expressing *E. coli* was clearly larger compared to their respective uninduced *E. coli* samples as shown in Fig. 1c. The lower cfu detected that were different from the uninduced control is found at 8×10^5 cfu with a $\Delta\%$ R_{ct} of 63.20 ± 12.18 for induced and 24.20 ± 8.78 for uninduced samples. Lower cfu samples showed similar values of $\Delta\%$ R_{ct} between analyte and uninduced samples. In comparison, the fluorescence assay (Fig. 1d) showed a detection limit of 8×10^6 cfu ($p \leq 0.001$). More dilute samples did not show significant differences between bacteria expressing YadA and uninduced bacteria and can thus be explained by non-specific binding to the well material. The difference in LOD between the two detection techniques was due to the fact that EIS provided more sensitivity and linear detection compared to the fluorescence assay, which provided a semiquantitative detection.

Collagen direct attachment biosensor

Polymer characterisation by electrodeposition CV profile and EIS. The optimised biosensor was constructed step-by-step from the bare gold working electrode to the fully constructed biosensor. This second sensor-fabrication route consisted of directly bonding the collagen to the POc through EDC/sulfo-NHS, which are well-known cross-linkers used for bioconjugation.[31] Each optimisation step was characterised by CV and EIS, thus allowing choice of the best parameters.

First, 1 mM to 250 mM octopamine in 10 mM PB pH 7.2 was assessed. Also 10 mM PB pH 7.2 alone was valuated to observe any potential component to take into consideration from the buffer. In addition, electrochemical characterisation of the bare electrode was also carried for the different POc concentrations, electropolymerisation was successfully achieved as observed from the oxidation peaks on the first cycle and the absence of peak in the second, indicating an irreversible oxidation in all cases (Fig. S2a and b†). Once each electrode was passivated with the corresponding POc concentration, EIS measurements were performed to evaluate impedance. As previously commented, the Nyquist semicircle diameter increased or decreased in accordance to how insulating or conductive the surface was. As observed in Fig. 2a the Nyquist plots diameter increased with polymer concentration until 5 mM POc. Then, for higher concentrations, the Nyquist semicircle size started decreasing us indicating a more conductive surface at higher concentrations. Therefore, EIS results suggest that the more efficient surface coating was at 5 mM POc.

In addition, CV was performed to corroborate the results obtained by EIS (Fig. 2b). Similarly, 5 mM POc appeared to be one of the most insulating with higher concentrations showed more conductive profiles, which is in line with the EIS analysis. Both EIS and CV results are in accordance with oxidation current observed in the electropolymerisation profiles (Fig. S2†).

Characterisation of EDC/sulfo-NHS crosslinking. EDC/sulfo-NHS were employed as cross-linker between the POc and the collagen. The use of these linkers creates an amide linkage between the primary amines of the POc and the carboxylic acid of the collagen. A protocol as described in section Biosensor fabrication and adapted from ref. 31 was employed. First, EDC and sulfo-NHS were dissolved in 50 mM MES pH 5.5. Then, collagen previously dissolved in 50

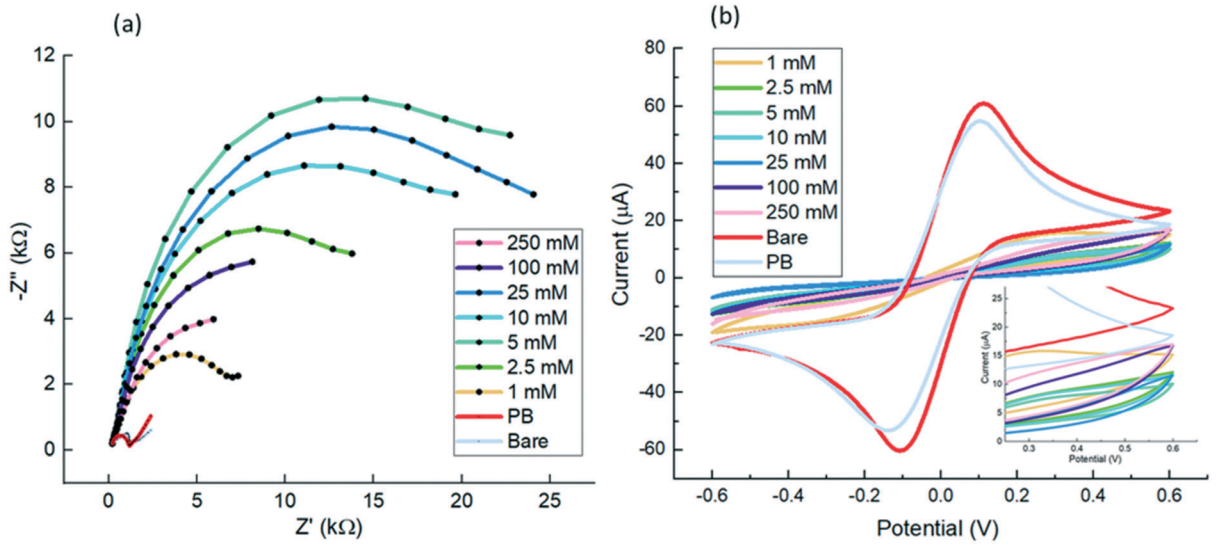

Fig. 2 Electrochemical characterisation of octopamine concentration. (a), Nyquist plot of bare, PB buffer and a range of POc concentrations, 1, 2.5, 5, 10, 25, 100, and 250 mM. All Nyquist profiles derived from EIS measurements in 10 mM $[Fe(CN)_6]^{3-/4-}$ in 10 mM PBS, pH 7.2, coupled to a potentiostat. EIS was recorded at 0 V over a frequency range of +5 kHz to +0.1 Hz, with a modulation voltage of +10 mV; (b), cyclic voltammogram of bare gold working electrode surface, PB buffer, and a range of POc concentrations, 1, 2.5, 5, 10, 25, 100 and 250 mM POc. The CV was cycled from −0.6 V to +0.6 at a scan rate of 100 mV s^{-1} in 10 mM $[Fe(CN)_6]^{3-/4-}$ in 10 mM PBS, pH 7.2.

mM MES pH 5.5 or in 10 mM acetic acid was added to the initial EDC/sulfo-NHS solution to yield in a final solution of 100 μg mL^{-1} collagen, 2 mM EDC and 6 mM sulfo-NHS in 50 mM MES pH 5.5. The solution was immediately placed over the POc coated surfaces and left for incubation for 2 h. After that, the electrodes were washed 3 times with 50 mM MES pH 5.5 and a final wash with 100 mM TRIS buffer in order to block any carboxylate reactive group left. The results shown in Fig. 3a indicate two very different profiles depending where the collagen was dissolved. Compared to the previous optimisation step in which 5 mM POc was optimum, the change on the Nyquist curve was larger when dissolving collagen in MES than in acetic acid. However, the Nyquist plot shown for MES as buffer showed less impedance than for acetic acid. The decrease in impedance could be a consequence of the polymer acting as a soft and stretchy net,

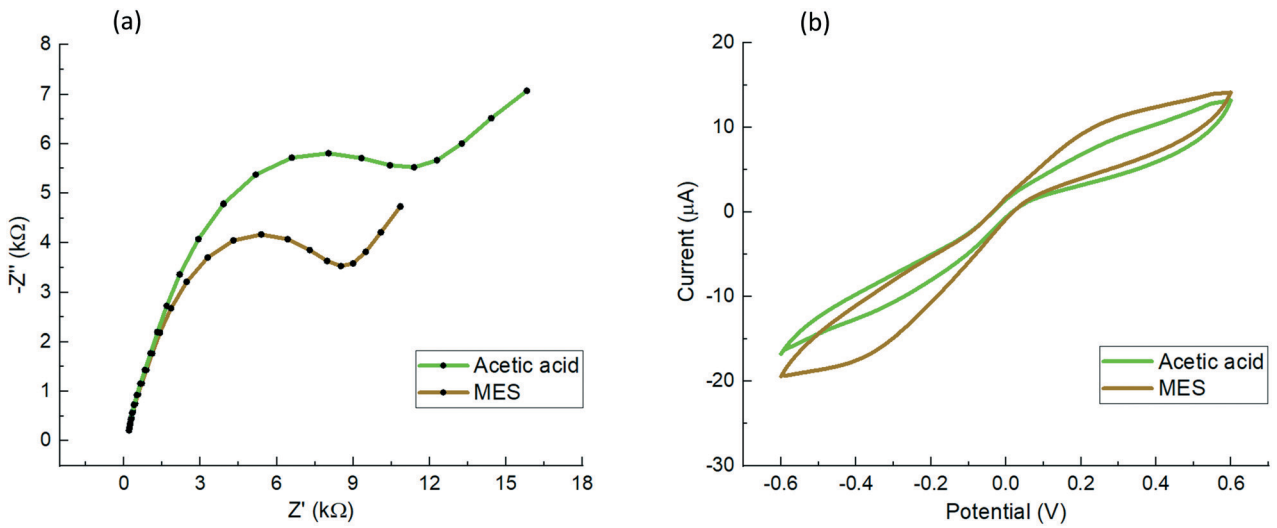

Fig. 3 Electrochemical characterisation of EDC/sulfo-NHS using two different protocols: direct immobilisation of 100 μg mL^{-1} collagen to 5 mM POc coated SPGEs was tested with two different protocols. In green, collagen dissolved in acetic acid prior to the addition to the EDC/sulfo-NHS solution in MES buffer; in brown, collagen was first dissolved in MES buffer to which later EDC/sulfo-NHS was added. (a), Nyquist plot representation. All Nyquist profiles derived from EIS measurements in 10 mM $[Fe(CN)_6]^{3-/4-}$ in 10 mM PBS, pH 7.2, coupled to a potentiostat. EIS was recorded at 0 V over a frequency range of +5 kHz to +0.1 Hz, with a modulation voltage of +10 mV; (b), the CV was cycled from −0.6 V to +0.6 at a scan rate of 100 mV s^{-1} in 10 mM $[Fe(CN)_6]^{3-/4-}$ in 10 mM PBS, pH 7.2.

when any attachment to it would distort the complex and create more space for the electron mediators to reach the electrode surface. This has been observed for other non-conducting polymers used in biosensors.[8] In line with the obtained results in EIS, the CV profiles (Fig. 3b) suggest that a more conductive surface can be found for the MES candidate whereas a more insulating surface was found for the acetic acid one.

Optimisation of collagen concentration. Assessment of the bioreceptor coating is crucial in any biosensor optimisation. In this biosensor, EDC/sulfo-NHS was employed to bind the POc amine groups to the carboxylic acid groups from the collagen. This direct attachment can yield semi-orientated collagen molecules as POc amine groups exist perpendicular to the surface. As explained in section Biosensor fabrication, collagen was dissolved in 50 mM MES pH 5.5, and ECD and sulfo-NHS were added to a final concentration of 2 mM EDC and 6 mM respectively. To avoid bioconjugate aggregation, the mixture was immediately placed onto the POc coated electrode surfaces and left for incubation. Different collagen concentrations, from 5 to 1000 μg mL^{-1} were assessed. From Fig. 4a, it can be observed that the increasing collagen concentrations were translated into a decrease in impedance. The Nyquist semicircles steadily decreased up to 100 μg mL^{-1}, and then higher concentrations only had a small impact on further impedance decrease. This behaviour was also observed in another study where non-conducting polymer was employed as the biosensor interface.[8] Similar to

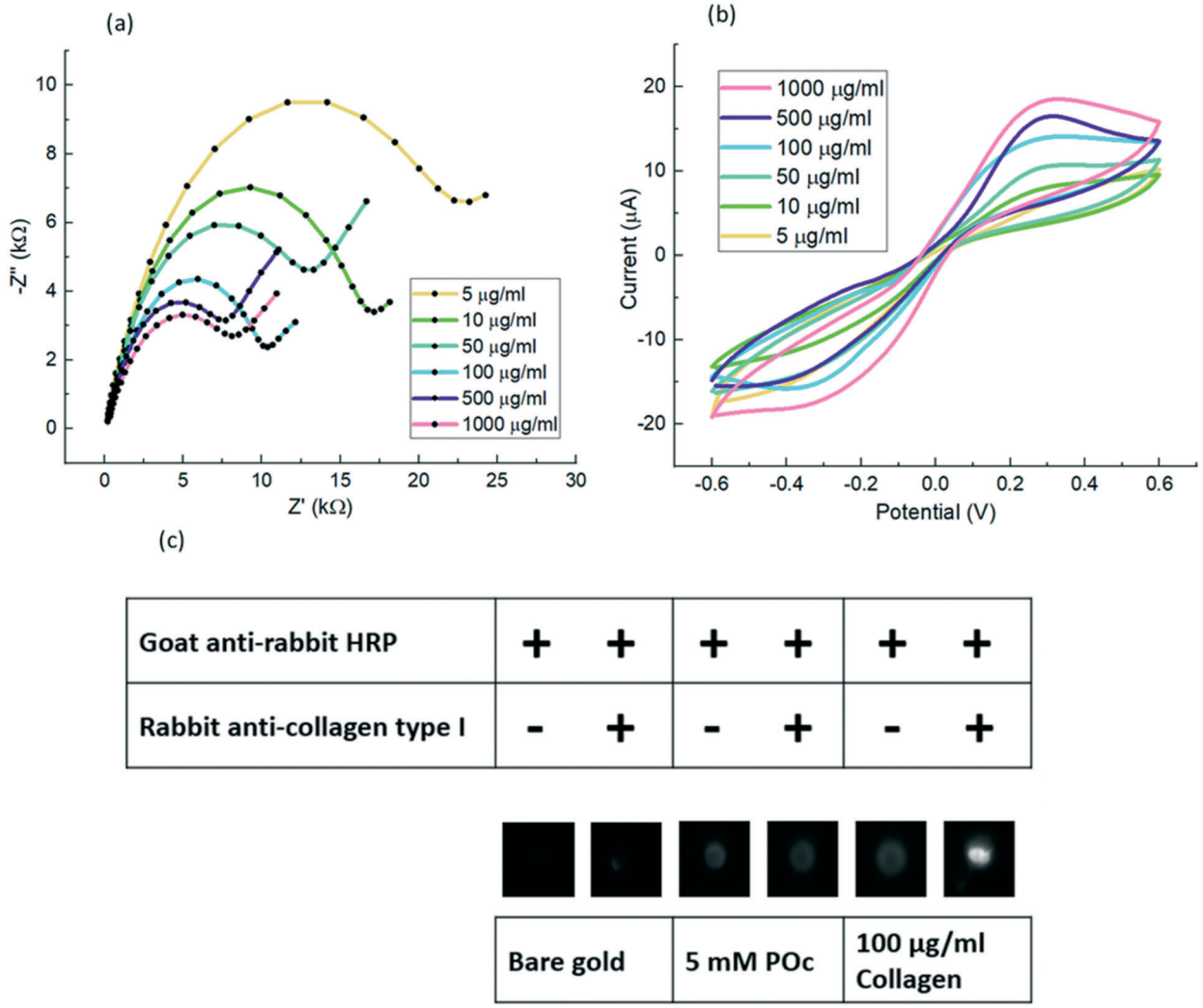

Fig. 4 Electrochemical characterisation of a different range of collagen concentrations and validation of collagen direct attachment to POc through on-sensor blotting: direct immobilisation of 5–1000 μg mL^{-1} of collagen to 5 mM POc *via* EDC/sulfo-NHS were tested and assessed by EIS and CV and finally validated with on-sensor blotting chemiluminescence. (a), All Nyquist profiles derived from EIS measurements were in 10 mM $[Fe(CN)_6]^{3-/4-}$ in 10 mM PBS, pH 7.2. EIS was recorded at 0 V over a frequency range of +5 kHz to +0.1 Hz, with a modulation voltage of +10 mV; (b), CVs were cycled from −0.6 V to +0.6 at a scan rate of 100 mV s^{-1} in 10 mM $[Fe(CN)_6]^{3-/4-}$ in 10 mM PBS, pH 7.2; (c), Midland blotting[29] was carried out to validate the collagen binding to POc. The sample was tested with 100 μg mL^{-1} collagen. Samples were prepared by adding primary rabbit anti-collagen type I, then addition of secondary goat anti-rabbit HRP antibodies as detailed in section Chemiluminescence analysis. Control samples comprised a bare gold surface, coated with 5 mM POc, or omission of primary antibodies as negative controls.

the EIS experiments, the CV profiles (Fig. 4b) showed increased intensity with increasing collagen concentration.

To validate the collagen direct attachment to POc through EDC/sulfo-NHS, one more experiment following the Midland blotting[29] technique was carried out as detailed in section Biosensor fabrication. As shown in Fig. 4c the presence of attached collagen was determined by on-sensor chemiluminescence in which two control surfaces were tested.

Optimisation of sample incubation time. The time needed for incubation sample was assessed using incubation times from 5 min to and 60 min. Here, YadA induced *E. coli* with 8×10^6 cfu bacteria in 10 μL sample were tested. From the Nyquist plot (Fig. 5), it is clear that 5 min incubation showed the lowest impedance and the signal substantially increased after 15 min. Thereafter, longer incubation times did not substantially affect the signal. It should be noted that the bacterial detection, in the final sensor, was manifested by an increase in impedance, unlike when adding collagen during fabrication.

Blocking agent. To further improve the selectivity and sensitivity of the biosensor, two possible blocking agents were considered. Either 1.5 mg mL^{-1} BSA or 1.5 mg mL^{-1} casein in 10 mM PBS were used to block the biosensor surface just before the analyte addition. Fully constructed biosensors were incubated with the corresponding blocking solution for 1 h. After that, the electrodes were washed with PBS buffer plus 0.05% Tween-20 and then 8×10^6 cfu in 10 μL of YadA induced or uninduced bacteria added.

As observed in Fig. 6, BSA and casein blocked surfaces showed bacterial binding (54.89 ± 12.93 and 41.31 ± 15.71 respectively) as substantial as the non-blocked surface (61.61 ± 7.80). However, the blocked biosensor variability was substantially larger than the unblocked one. When control samples were tested with uninduced bacteria, it was observed that the BSA and casein blocked surfaces showed less non-specific binding, 11.45 ± 10.25 and 9.87 ± 13.31 respectively, compared to the non-blocked surface, 26.12 ± 5.95. Nonetheless, the variability of the control samples were substantially larger than the samples without blocking agent and therefore a blocking step was not deemed essential for this work.

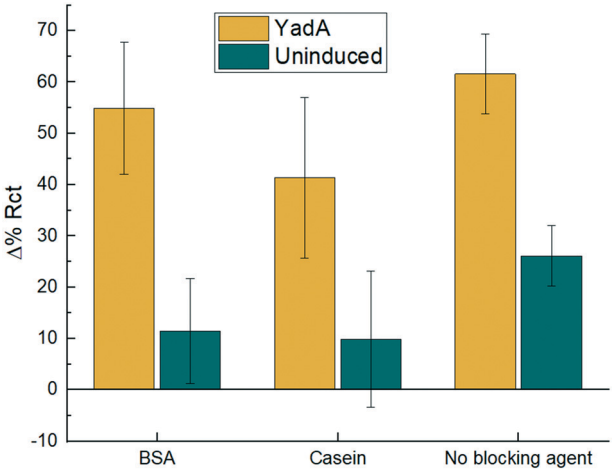

Fig. 6 Electrochemical binding measurements for blocked and non-blocked biosensors. 1.5 mg mL^{-1} BSA, 1.5 mg mL^{-1} casein and non-blocked biosensor were tested with 8×10^6 cfu in 10 μL sample for *E. coli* expressing YadA or uninduced *E. coli*. Incubation was for 15 min and Δ% R_{ct} is calculated with eqn (1). Data are mean ± SD (n = 6).

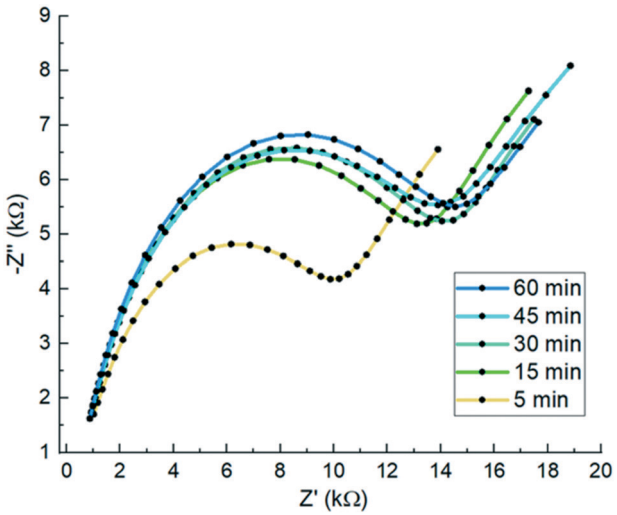

Fig. 5 Electrochemical characterisation of different incubation times. Different incubation times were assessed for 5, 15, 30, 45, and 60 min incubation. The sensors were left incubating with 8×10^6 cfu in 10 μl sample of YadA induced *E. coli*. All Nyquist profiles derived from EIS measurements in 10 mM $[Fe(CN)_6]^{3-/4-}$ in 10 mM PBS, pH 7.2 and were recorded at 0 V over a frequency range of +5 kHz to +0.1 Hz, with a modulation voltage of +10 mV.

Bacterial detection. Finally, a fully step-by-step optimised biosensor was assessed for bacterial detection. A concentration of 5 mM POc, 100 μg ml^{-1} of collagen dissolved in 50 mM MES pH 5.5 with EDC/sulfo-NHS added, without blocking steps, was used to detect bacterial samples after 15 min of incubation. For that, *E. coli* samples expressing YadA and control, using uninduced *E.coli*, were tested for bacterial samples ranging from 8×10^2 to 8×10^7 cfu in 10 μL PBS media sample. The samples were incubated for 15 min on the biosensor and washed out with PBS prior to analysis.

From the bar chart (Fig. 7), it can be observed that the two lowest bacterial concentrations of 8×10^2 and 8×10^3 cfu were not detected. From 8×10^4 cfu with Δ% R_{ct} 38.98 ± 3.04 for YadA induced and 15.20 ± 4.95 for uninduced, to larger cfu samples, there was a differentiated analyte response proportional to concentration. Sensors challenged with YadA induced bacteria (Fig. 7) showed a steady increase in % ΔR_{ct}. However, higher bacterial concentrations gave greater variability. The trend shown in the bar graphs appear to show a plateau in response for uninduced samples. The biosensors also tested bacteria over the polymer in absence of collagen. No significant binding was observed (Fig. S3†).

Conclusions

In this study, we present collagen as a bioreceptor for a proof-of-concept impedance-based biosensor for rapid

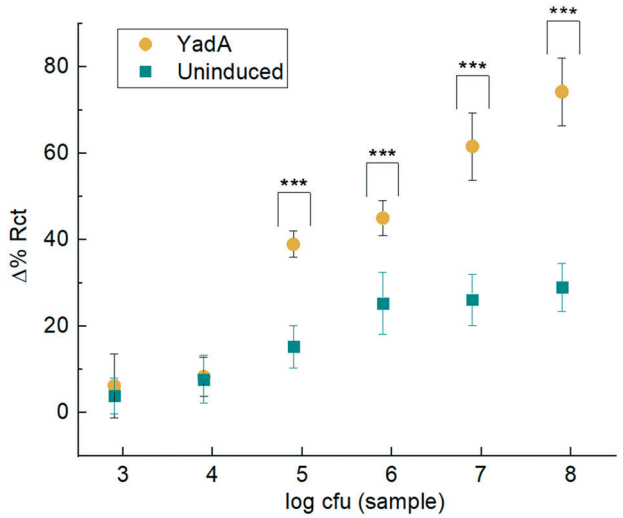

Fig. 7 Electrochemical binding measurements. Δ% R_{ct} before and after analyte incubation with uninduced *E. coli* or *E. coli* expressing YadA for a range of bacteria from 8×10^2 to 8×10^7 cfu in 10 μL. Incubation was for 15 min and Δ% R_{ct} is calculated in accordance with eqn (1). Data are mean ± SD ($n \geq 6$). Statistical analysis was performed using ANOVA and data with $p < 0.001$ are indicated by ***.

bacterial measurement. The first system, based on a non-optimised polymer-collagen matrix bioreceptor, can detect 8×10^5 cfu to 8×10^7 cfu in 10 μL sample of YadA expressing *E. coli*. The second system, based on an optimised direct attachment of the collagen, can detect 8×10^4 cfu to 8×10^7 cfu in 10 μL sample of YadA expressing *E. coli*. The aim of this research was to demonstrate that the ECM protein–adhesin interaction can be utilized for detection of whole pathogens using an electrochemical biosensor. In addition, ECM proteins utilised as bioreceptors could offer pan-specificity, *i.e.* the biosensor could detect a group of organisms rather than a specific organism. This first-step determination could be a useful tool for clinicians who need to perform a rapid initial 'sample in, answer out' diagnostic test in order to begin treatment, before the lengthier investigation of identifying exact species. In contrast, antibody-based biosensors may be too specific for a certain pathogen and may miss the detection of other species. A balance of the specificity of these models will provide more accurate diagnostic results for clinicians.

Analogous to YadA used as a model surface adhesin in this study, all pathogenic bacteria have adhesins targeting host cell structures.[17,18] As adhesins generally show specificities for different targets, this could in the future be harnessed for diagnostic purposes as previously discussed. A potential device could use panels of biosensors coated with different ECM molecules and host surface structures to identify pathogenic bacteria based on their adhesion patterns. Other common electrochemical biosensors, for instance, can detect *E. coli* at a concentration of 1.4×10^3 cfu mL^{-1} in 25 μL sample[32] or other bacteria species such as *S. typhimurium* at a concentration of 10^3 cfu mL^{-1} in 1 mL,[33] or *S. pyogenes* detecting 100 cells in 10 μL.[8] While this method will likely not replace more accurate methods like mass spectrometry, a biosensor-based approach could function as an initial, rapid point- of-care device for what type of infection is present. In contrast to other methods, biosensor-based methods do not require growth of the pathogen on plates.[34,35] While slightly less accurate, biosensors coated with ECM molecules rather than antibodies or enzymes would be less expensive in comparison.

Author contributions

J. Leva-Bueno: investigation, writing – original draft, visualisation. I. Meuskens: validation, writing – original draft, visualisation. D. Linke: conceptualisation, writing – review & editing, supervision. P. A. Millner: conceptualisation, writing – review & editing, supervision, project administration. S. A. Peyman: conceptualisation, writing – review & editing, supervision, project administration.

Conflicts of interest

There are no conflicts to declare.

Acknowledgements

Funding: this project is funded by the European Union's Horizon 2020 Research and Innovation Programme under the Marie Skłodowska-Curie grant agreement No. 765042. D. Linke also receives funding from the Center for Digital Life, grant 294605 (Research Council of Norway). The data repository for this publication is available at **https://doi.org/10.5518/1165**.

Notes and references

1 H. W. Boucher, *et al.*, Bad bugs, no drugs: No ESKAPE! An update from the Infectious Diseases Society of America, *Clin. Infect. Dis.*, 2009, **48**, 1–12.
2 M. Gajdács and F. Albericio, Antibiotic resistance: from the bench to patients, *Antibiotics*, 2019, **8**, 8–11.
3 A. Cassini, *et al.*, Attributable deaths and disability-adjusted life-years caused by infections with antibiotic-resistant bacteria in the EU and the European Economic Area in 2015: a population-level modelling analysis, *Lancet Infect. Dis.*, 2019, **19**, 56–66.
4 C. K. Joung, *et al.*, Ultra-sensitive detection of pathogenic microorganism using surface-engineered impedimetric immunosensor, *Sens. Actuators, B*, 2012, **161**, 824–831.
5 J. Leva-Bueno, S. A. Peyman and P. A. Millner, A review on impedimetric immunosensors for pathogen and biomarker detection, *Med. Microbiol. Immunol.*, 2020, **209**, 343–362.
6 Z. Taleat, A. Khoshroo and M. Mazloum-Ardakani, Screen-printed electrodes for biosensing: A review (2008-2013), *Microchim. Acta*, 2014, **181**, 865–891.
7 M. Xu, R. Wang and Y. Li, Electrochemical biosensors for rapid detection of Escherichia coli O157:H7, *Talanta*, 2017, **162**, 511–522.

8 A. Ahmed, J. V. Rushworth, J. D. Wright and P. A. Millner, Novel impedimetric immunosensor for detection of pathogenic bacteria streptococcus pyogenes in human saliva, *Anal. Chem.*, 2013, **85**, 12118–12125.
9 J. R. Birch and A. J. Racher, Antibody production, *Adv. Drug Delivery Rev.*, 2006, **58**, 671–685.
10 Y. Chen, *et al.*, Recent advances in rapid pathogen detection method based on biosensors, *Eur. J. Clin. Microbiol. Infect. Dis.*, 2018, **37**, 1021–1037.
11 E. Cesewski and B. N. Johnson, Electrochemical biosensors for pathogen detection, *Biosens. Bioelectron.*, 2020, **159**, 112214.
12 Q. Wu, Y. Zhang, Q. Yang, N. Yuan and W. Zhang, Review of electrochemical DNA biosensors for detecting food borne pathogens, *Sensors*, 2019, **19**(22), 4916.
13 F. Xi, J. Gao, J. Wang and Z. Wang, Discrimination and detection of bacteria with a label-free impedimetric biosensor based on self-assembled lectin monolayer, *J. Electroanal. Chem.*, 2011, **656**, 252–257.
14 A. Shabani, *et al.*, Bacteriophage-modified microarrays for the direct impedimetric detection of bacteria, *Anal. Chem.*, 2008, **80**, 9475–9482.
15 H. Jafari, *et al.*, Entrapment of uropathogenic E. coli cells into ultra-thin sol-gel matrices on gold thin films: A low cost alternative for impedimetric bacteria sensing, *Biosens. Bioelectron.*, 2019, **124–125**, 161–166.
16 S. Xia, *et al.*, Development of a simple and convenient cell-based electrochemical biosensor for evaluating the individual and combined toxicity of DON, ZEN, and AFB1, *Biosens. Bioelectron.*, 2017, **97**, 345–351.
17 I. Meuskens, A. Saragliadis, J. C. Leo and D. Linke, Type V secretion systems: An overview of passenger domain functions, *Front. Microbiol.*, 2019, **10**, 1–19.
18 B. Westerlund and T. K. Korhonen, Bacterial proteins binding to the mammalian extracellular matrix, *Mol. Microbiol.*, 1993, **9**, 687–694.
19 J. Pizarro-Cerdá and P. Cossart, Bacterial adhesion and entry into host cells, *Cell*, 2006, **124**, 715–727.
20 J. C. Leo, H. Elovaara, B. Brodsky, M. Skurnik and A. Goldman, The Yersinia adhesin YadA binds to a collagenous triple-helical conformation but without sequence specificity, *Protein Eng., Des. Sel.*, 2008, **21**, 475–484.
21 M. Mühlenkamp, P. Oberhettinger, J. C. Leo, D. Linke and M. S. Schütz, Yersinia adhesin A (YadA) - Beauty & beast, *Int. J. Med. Microbiol.*, 2015, **305**, 252–258.
22 H. Nummelin, Y. El Tahir, P. Ollikka, M. Skurnik and A. Goldman, Expression, purification and crystallization of a collagen-binding fragment of Yersinia adhesin YadA, *Acta Crystallogr., Sect. D: Biol. Crystallogr.*, 2002, **58**, 1042–1044.
23 D. Linke, T. Riess, I. B. Autenrieth, A. Lupas and V. A. J. Kempf, Trimeric autotransporter adhesins: variable structure, common function, *Trends Microbiol.*, 2006, **14**, 264–270.
24 Y. El Tahir and M. Skurnik, YadA, the multifaceted Yersinia adhesin, *Int. J. Med. Microbiol.*, 2001, **291**, 209–218.
25 J. C. Leo, *et al.*, First analysis of a bacterial collagen-binding protein with collagen toolkits: Promiscuous binding of YadA to collagens may explain how YadA interferes with host processes, *Infect. Immun.*, 2010, **78**, 3226–3236.
26 H. Nummelin, *et al.*, The Yersinia adhesin YadA collagen-binding domain structure is a novel left-handed parallel β-roll, *EMBO J.*, 2004, **23**, 701–711.
27 A. Saragliadis and D. Linke, Assay development for the discovery of small-molecule inhibitors of YadA adhesion to collagen, *Cell Surf.*, 2019, **5**, 100025.
28 U. Grosskinsky, *et al.*, A conserved glycine residue of trimeric autotransporter domains plays a key role in Yersinia adhesin A autotransport, *J. Bacteriol.*, 2007, **189**, 9011–9019.
29 J. V. Rushworth, A. Ahmed and P. A. Millner, Midland Blotting: A Rapid, Semi-Quantitative Method for Biosensor Surface Characterization, *J. Biosens. Bioelectron.*, 2013, **4**, 146.
30 S. H. Shamsuddin, *et al.*, Reagentless Affimer- and antibody-based impedimetric biosensors for CEA-detection using a novel non-conducting polymer, *Biosens. Bioelectron.*, 2021, **178**, 113013.
31 G. T. Hermanson, *Bioconjugate Techniques*, Elsevier, 1996.
32 R. Wang, *et al.*, A label-free impedance immunosensor using screen-printed interdigitated electrodes and magnetic nanobeads for the detection of E. coli O157:H7, *Biosensors*, 2015, **5**, 791–803.
33 Z. Farka, *et al.*, Rapid Immunosensing of Salmonella Typhimurium Using Electrochemical Impedance Spectroscopy: the Effect of Sample Treatment, *Electroanalysis*, 2016, **28**, 1803–1809.
34 A. Croxatto, G. Prod'hom and G. Greub, Applications of MALDI-TOF mass spectrometry in clinical diagnostic microbiology, *FEMS Microbiol. Rev.*, 2012, **36**, 380–407.
35 B. W. Senior, Media and tests to simplify the recognition and identification of members of the Proteeae, *J. Med. Microbiol.*, 1997, **46**, 39–44.